

# Pulsed VHE emission from the Crab Pulsar in the context of magnetocentrifugal particle acceleration.

Z. Osmanov,<sup>1\*</sup> & F.M. Rieger<sup>2,3†</sup>

<sup>1</sup>*School of Physics, Free University of Tbilisi, 0183, Tbilisi, Georgia*

<sup>2</sup>*Zentrum für Astronomie (ZAH), Institut für Theoretische Astrophysik, Universität Heidelberg, Philosophenweg 12, 69120 Heidelberg*

<sup>3</sup>*Max-Planck-Institut für Kernphysik, P.O. Box 103980, 69029 Heidelberg, Germany*

20 September 2016

## ABSTRACT

The Crab Pulsar has been recently detected at very high energies (VHE) with its pulsed VHE emission reaching up to 1.5 TeV. The VHE peaks appear synchronised with the peaks at GeV energies and show VHE spectra following hard power-law functions. These new findings have been interpreted as evidence for a gamma-ray production that happens very close to the light cylinder. Motivated by these experimental results we consider the efficiency of magnetocentrifugal particle acceleration in the magnetosphere of the Crab Pulsar, reexamining and extending results obtained in a previous work (Osmanov & Rieger 2009). It is shown that efficient magnetocentrifugal acceleration close to the light cylinder could provide the required electron Lorentz factors of  $5 \times 10^6$  and that the resulting inverse Compton (IC) scattering off thermal photons might explain the enigmatic TeV emission of the pulsar. We estimate the corresponding VHE luminosity and provide a derivation of its spectral characteristics, that appear remarkably close to the observational results to encourage further studies.

**Key words:** acceleration of particles - MHD - pulsars: general - pulsars: individual: Crab Pulsar

## 1 INTRODUCTION

Rotating neutron stars are today known to be accompanied by pulsed non-thermal high- and very high energy (VHE) gamma-ray emission (e.g., Abdo et al. 2013; Lemoine-Goumard 2015). While these observations point to the presence of highly energetic charged particles in the pulsar environment, the origin of these particles is still an open question (see e.g., Aharonian et al. 2012; Bednarek 2012; Hirotani 2014; Harding & Kalapotharakos 2015; Mochol & Pétri 2015).

According to the standard theory of pulsars, primary particles are uprooted from the star's surface by means of strong longitudinal (along the magnetic field line) electrostatic fields (Ruderman & Sutherland 1975) and efficiently accelerated in a region between the surface and the light cylinder (LC) area (a hypothetical zone where the linear velocity of rotation matches the speed of light). In order to produce VHE emission up to TeV energies, as e.g. seen in the case of the Crab Pulsar, electrons would need to achieve high Lorentz factors of the order of  $\sim 10^6 - 10^7$  (e.g., Aliu et al. 2011; Ansoldi et al. 2016).

It is still not known which mechanism of acceleration is responsible for that and where in the magnetosphere this process may take place. In the framework of e.g. polar cap models longitudinal electrostatic fields are presumed to allow significant particle acceleration along open magnetic field lines close to the neutron star (e.g., Arons 1983; Michel 1991). However, the acceleration efficiency is usually found to be too strongly limited by curvature and/or Inverse Compton radiation processes (Daugherty & Harding 1982; Dermer & Sturmer 1994) in order to account for the production of TeV particles. To overcome these difficulties, alternative (so-called outer gap) models might be invoked (e.g., Cheng et al. 1986; Chiang & Romani 1994; Hirotani 2007), where particles are accelerated in the outer parts of the magnetosphere. Yet the anticipated radiation reaction forces along with the relatively short gap sizes still impose severe constraints on maximum attainable particle energies. A number of different approaches have been considered to improve on these problems. Usov & Shabad (1985) for example, have examined the intermediate formation of an electron-positron bound state that could possibly prevent an early screening of the gap electric field. Muslimov & Tsygan (1992), on the other hand, have extended the pulsar's electrodynamics by taking into account general relativistic effects. Although these mechanisms allowed to slightly in-

\* E-mail: z.osmanov@astro-ge.org

† E-mail: frank.rieger@mpi-hd.mpg.de

crease the gap size and thus led to more energetic particles, the corresponding energies are still not high enough when put in the context of recent VHE observations.

In general, the pulsar magnetosphere is characterized by extremely strong magnetic fields, which in the case of the Crab Pulsar are believed to be of the order of  $4 \times 10^{12}$  G close to star's surface. This in turn means that charged particles very efficiently emit synchrotron radiation with an associated cooling timescale  $t_{syn} \sim \gamma m_0 c^2 / P_{syn}$  (where  $\gamma$ ,  $m_0$  is the electron's Lorentz factor and mass, respectively,  $c$  is the speed of light,  $P_{syn} \approx 2e^4 \gamma^2 B^2 / 3m_0^2 c^3$  is the single particle synchrotron power and  $e$  is the electron's charge) that is by many orders of magnitude smaller than the kinematic timescale  $P$ , where  $P$  is the rotation period, i.e.  $P \approx 0.0334$  sec in the case of the Crab Pulsar (e.g., Lyne et al. 2015). Hence, charged particles injected into the magnetosphere will quickly transit to the ground Landau level and start sliding along the magnetic field lines. As the field lines co-rotate with the star, the particle dynamics is then expected to be strongly influenced by the effects of centrifugal acceleration and the synchrotron losses do not impose constraints on the maximum attainable energies of particles.

It is clear that these effects might be extremely efficient close to the LC zone. In the context of the Crab, the possible role of the centrifugal mechanism to generate the pulsar's emission has been examined by Gold (1969). In particular, he has argued that the co-rotation of plasma particles in the pulsar's magnetosphere could "create" an efficient energy transfer channel from the rotator into the kinetic energy of plasma particles. Motivated by this, a simplified model of centrifugal acceleration was developed by Machabeli & Rogava (1994), who considered a rectilinear rotating channel with a body, freely sliding inside it. In the framework of special relativity they showed for the first time that the incorporation of relativistic effects of rotation can lead to radial deceleration, which is at first sight a rather uncommon phenomenon, yet already known from general relativity (Abramowicz & Prasanna 1990).

Since then, centrifugal particle acceleration has been studied in a variety of contexts and used to e.g., predict the location to frequency mapping in the case of multi-second pulsars (Gangadhara 1996; Thomas & Gangadhara 2007) or to analyse the origin of the variable high energy emission from the rotating jet base in active galactic nuclei (AGN) (e.g., Gangadhara & Lesch 1997; Rieger & Mannheim 2000; Xu 2002; Osmanov et al. 2007; Ghisellini et al. 2009). The results illustrated amongst other the particular role of inverse Compton scattering on the efficiency of centrifugal acceleration. In a direct application of centrifugal acceleration to Crab-like pulsars we have shown that close to the LC area electrons could achieve Lorentz factor up to  $\gamma \sim 10^7$  (Osmanov & Rieger 2009). The analysis of different radiation processes suggested that inverse Compton scattering in the Crab Pulsar's magnetosphere could lead to detectable pulsed VHE emission in the TeV band.

Based on the MHD approximation, a detailed investigation of magneto-centrifugal acceleration of plasma bulk motion close to the light cylinder has been recently presented by Bogovalov (2014), extending an earlier approach developed in Bogovalov (2001). The results are of particular interest as they lead to very similar expectations in the case of the Crab Pulsar. In that approach the dynamics of the parti-

cles has been investigated for different 3dim-configuration of magnetic field lines and it was shown that close to the LC area particles can achieve extremely high Lorentz factor following a scaling as previously employed.

The aforementioned works are especially interesting in the context of the latest results by the MAGIC Collaboration reporting the detection of pulsed VHE emission up to 1.5 TeV from the Crab Pulsar, the highest ever detected (Ansoldi et al. 2016). The VHE pulse profiles revealed two narrow peaks P1 (located at a phase close to 1) and P2 (located at a phase close to 0.4) that appear synchronised with those seen by Fermi-LAT in the GeV domain. Their detection significance (in  $\sim 320$ h of data) is different, though, with only P2 being significantly detected ( $> 5\sigma$ ) at energies above 400 GeV. The phase-folded pulse spectra are compatible with power-law functions over a range of  $\sim 70$  GeV up to 1.5 TeV, with photon indices  $\alpha = 3.5 \pm 0.1$  (for P1) and  $\alpha = 3.0 \pm 0.1$  (for P2), and TeV flux levels  $E^2 dN/dEdAdt \lesssim 5 \times 10^{-14}$  TeV cm $^{-2}$ s $^{-1}$  (P1) and  $(9 \pm 3) \times 10^{-14}$  TeV cm $^{-2}$ s $^{-1}$  (P2), respectively. It is worth noting that this is the first clear detection of a pulsed emission component from the Crab in the TeV regime. Unpulsed (steady) TeV emission, attributed to its nebula, has been detected quite some time ago (e.g., Weekes et al. 1989; Aharonian et al. 2004) whereas early evidence for pulsed gamma-ray emission (above a few tens of GeV) has been related to an inverse Compton (IC) origin in the pulsar wind zone some tens of light cylinder radii away (Aharonian et al. 2012).

In this paper we reconsider the role of the magneto-centrifugal acceleration for the Crab Pulsar in the light of the latest VHE findings, applying and extending results previously obtained (Osmanov & Rieger 2009). We show that the agreement with observations is successfully close to encourage further modelling. The paper is organized in the following way. In section II, basic results of centrifugal acceleration are recaptured and discussed. Section III then presents an application to the Crab Pulsar, while conclusions are summarised in section IV.

## 2 CENTRIFUGAL ACCELERATION

### 2.1 Energy-Position Dependence

In this section we consider the dynamics of centrifugally accelerated particles close to the LC surface. As noted above, synchrotron losses will ensure that a charge particle quickly transits to the ground Landau level and starts to slide along the field line. Under such conditions it can be shown that the Lagrangian of a single relativistic massive particle (with rest mass  $m_0$ ) moving along a co-rotating field line located in the equatorial plane can be written as (Rieger 2011)

$$L = -m_0 (1 - v_r^2 - v_\phi^2)^{1/2}, \quad (1)$$

where ( $c \equiv 1$ ),  $v_r = \dot{r}$  and  $v_\phi = \Omega r + \dot{r} B_\phi / B_r$  are respectively the radial and tangential components of velocity,  $\Omega = 2\pi/P$  is the pulsar's angular velocity of rotation, and  $B_r$  and  $B_\phi$  are the corresponding components of the magnetic field, respectively. Since the Lagrangian is not explicitly time-dependent, the related Hamiltonian  $H = \dot{r}P - L$ , where  $P = \partial L / \partial \dot{r}$  is the generalized momentum, is a constant of motion (Noether's theorem). Using Eq. (1) one finds

$$H = \gamma m_0 (1 - \Omega r v_\phi) = \text{const}, \quad (2)$$

Accordingly, in the presence of a dominant radial field, the radial behaviour of the Lorentz factor for a particle injected at  $r_0$  with initial Lorentz factor  $\gamma_0$  becomes (Rieger 2011)

$$\gamma(r) = \gamma_0 \frac{(1 - r_0^2/r_L^2)}{(1 - r^2/r_L^2)}, \quad (3)$$

where  $r_L = c/\Omega$  denotes the light cylinder radius. A charged particle following the field will thus dramatically increase its Lorentz factor upon approaching the light cylinder ( $r \rightarrow r_L$ ). Using eq. (3) and the general definition of  $\gamma$ , the characteristic acceleration timescale can be expressed as

$$t_{\text{acc}}(\gamma) = \frac{\gamma}{\dot{\gamma}} \simeq \frac{\gamma_0^{1/2} (1 - r_0^2/r_L^2)^{1/2} r_L}{2\gamma^{1/2} c} \propto 1/\sqrt{\gamma} \quad (4)$$

In principle, the Lorentz factor dependence, eq. (3), can also be obtained within the fluid dynamical framework of the MHD approximation. As shown recently by Bogovalov (2014), the relativistic dynamics of particles following a rotating field line with a general 3d-shape in a plasma satisfying the frozen-in condition obeys the equation

$$\frac{1}{\gamma} \frac{\partial \gamma}{\partial R} = \frac{2R}{1 - R^2} + \frac{v_r (v^2 \cos \psi + R (1 - R^2) \frac{\partial \cos \psi}{\partial R})}{(1 - R^2) (\mathbf{e}_r \mathbf{e}_B) (1 - v_d^2)}, \quad (5)$$

where  $R = r/r_L$  is the dimensionless radial coordinate,  $v$  is the total particle velocity,  $\mathbf{e}_r$  and  $\mathbf{e}_B$  are the unit vectors along the radial coordinate and along the direction of the magnetic field line, respectively,  $\psi$  is the angle between  $\mathbf{e}_r$  and  $\mathbf{e}_\phi$ ,  $\mathbf{e}_\phi$  is the unit tangential vector,  $v_d = \mathbf{E} \times \mathbf{B}/B^2$  is the drift velocity and  $\mathbf{E}$  and  $\mathbf{B}$  are the electric and magnetic field vectors, respectively. As discussed by Bogovalov (2014), on approaching the LC ( $R = 1$ ) the second term of the right-hand side of Eq. (5) remains finite, while the first term diverges. Therefore, the aforementioned equation reduces to

$$\frac{1}{\gamma} \frac{\partial \gamma}{\partial R} = \frac{2R}{1 - R^2}, \quad (6)$$

which no longer depends on the concrete shape of the field line (as long as it is positively twisted) and has the solution expressed in eq. (3). Identifying possible sites in numerical simulations and adopting parameters characteristic for the Crab Pulsar, Bogovalov (2014) found that Lorentz factor up to  $\sim 5 \times 10^7$  (at the Alfvénic surface) could be achieved by magnetocentrifugal acceleration.

## 2.2 Trajectories - the Archimedean spiral as attractor

On crossing the light cylinder, magnetic field lines frozen into the plasma are generally expected to approach an Archimedean spiral shape with the plasma flowing in it at constant Lorentz factor, i.e. the Archimedean spiral becomes an attractor (Bogovalov 2014). This compares well with the analysis of Rogava et al. (2003) who, in an extension of the work by Machabeli & Rogava (1994), examined curved rotating channels in the equatorial plane and studied the relativistic dynamics of a particle sliding inside this channel. As seen by a laboratory observer, the effective angular velocity of a particle can be written as (Rogava et al. 2003)

$$\Omega_{\text{ef}} = \Omega + \phi'(r) v_r, \quad (7)$$

where the shape of the channel is given in polar coordinates in terms of  $\phi$ . On the other hand, since we observe plasma particles escaping the inner magnetosphere, the particle dynamics is expected to tend to the force-free regime. As a consequence the effective angular velocity has to vanish eventually and the particle's radial velocity should saturate. This in turn means that the physically interesting "trajectories" are those with  $\phi(r) = ar$ , where  $a$  is a constant. Together with  $\Omega$  this explicitly defines the asymptotic velocity as

$$v_{as} = -\frac{\Omega}{a}. \quad (8)$$

Obviously, if the initial velocity of the particle coincides with  $v_{as}$ , its dynamics will be force-free from the very beginning. It seems interesting to study what happens if the initial velocities are different. For this purpose one can consider the metric tensor on the Archimedean field lines (Rogava et al. 2003)

$$ds^2 = g_{00} dt^2 + 2g_{01} dt dr + g_{11} dr^2, \quad (9)$$

where

$$g_{\alpha\beta} = \begin{pmatrix} -(1 - \Omega^2 r^2), & a\Omega r \\ a\Omega r, & 1 + a^2 r^2 \end{pmatrix}, \quad (10)$$

with indices  $\alpha, \beta = 0, 1$  and using  $c \equiv 1$ . Then, by introducing the Lagrangian of a particle (e.g., Shapiro & Teukolsky 2004)

$$L_A = -m_0 \left( g_{\alpha\beta} \frac{dx^\alpha}{d\tau} \frac{dx^\beta}{d\tau} \right)^{1/2}, \quad (11)$$

one can see that  $t$  is a cyclic parameter for which the associated conjugate momentum is conserved. Therefore, one can show that the proper energy of the particle (per unit rest mass) given by

$$E_A = -\frac{g_{00} + g_{01} v_r}{(-g_{00} - 2g_{01} v_r - g_{11} v_r^2)^{1/2}}, \quad (12)$$

is a conserved quantity. Here we have employed the fact that based on the normalisation of the 4-velocity, the Lorentz factor of the particle in terms of the radial velocity is given by  $\gamma(r) = (-g_{00} - 2g_{01} v_r - g_{11} v_r^2)^{-1/2}$ . Equation (12) then leads to the following relation for the radial velocity

$$v_r = \frac{\sqrt{g_{00} + E_A^2}}{g_{01}^2 + E_A^2 g_{11}} \times \left[ -g_{01} \sqrt{g_{00} + E_A^2} \pm E_A \sqrt{g_{01}^2 - g_{00} g_{11}} \right]. \quad (13)$$

In Fig. 1 the characteristic behaviour of  $\gamma(r)$  is shown for different initial conditions. For illustration and in order to facilitate a comparison with Bogovalov (2014), a small (asymptotic) Lorentz factor  $\gamma_{as} = 7$  has been employed for the Archimedean spiral. As can be seen, even if the particles are initially not in the force-free regime, they asymptotically tend to it. A similar investigation but for 3-dim geometry has been recently performed by Gudavadze et al. (2015).

In Bogovalov (2014) it has been argued that efficient magnetocentrifugal acceleration occurs close to the Alfvénic region (an area where the Alfvénic velocity equals that of plasma particles). By estimating the corresponding distance in the case of the Crab Pulsar and using eq. (3) a maximum attainable value for the Lorentz factor,  $\gamma_{max} \sim 5 \times 10^7$

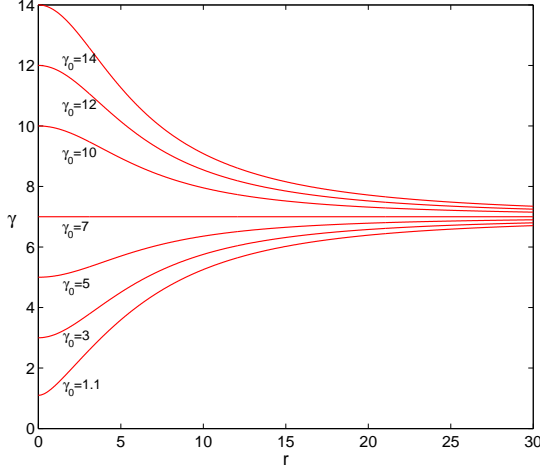


**Figure 1.** Characteristic dependence of the Lorentz factor on the radial coordinate for different initial Lorentz factors  $\gamma_0$ . For illustration the calculations are done for an Archimedean spiral with small (asymptotic) Lorentz factor  $\gamma_{as} = 7$ . All particles are launched from  $r_0 = 0$ . As it is evident from the plot, the curve  $\gamma = \gamma_{as}$  "attracts" all other curves.

has been inferred. As discussed in Osmanov & Rieger (2009) and considered in more detail in the following, the aforementioned value could in principle be slightly reduced by means of energy losses.

### 3 EMISSION CHARACTERISTICS

In the envisaged scenario, centrifugal particle acceleration can occur as long as the inertia of the plasma particles does not counteract efficient co-rotation with the magnetic field. This is satisfied if the magnetic field energy density  $B^2/8\pi$  exceeds the plasma energy density,  $\gamma n_{GJ} M m_0 c^2$ , where  $n_{GJ} = \Omega B \cos \alpha / (2\pi e c)$  is the Goldreich-Julian number density (Goldreich & Julian 1969) close to the star, i.e. the number density of primary particles,  $M \approx \gamma/\gamma_0$  is the multiplicity factor (Osmanov & Rieger 2009) and  $\alpha$  is the inclination angle between the axis of rotation and the magnetic dipole. For the Crab Pulsar one has  $P = 2\pi/\Omega = 0.033$  sec, a nominal light cylinder scale  $r_L = cP/2\pi = 1.58 \times 10^8$  cm, an effective radial distance  $r_l = r_L / \sin \alpha$  and a surface magnetic field  $B_0 \simeq 4 \times 10^{12}$  G. For a dipolar field approximation, the magnetic field then scales as  $B(r_l) \simeq 1.5 \times 10^6 \sin^3 \alpha$  G in the LC area. For these parameters, the requirement of efficient co-rotation leads to a constraint on the maximum Lorentz factor of

$$\gamma_{max}^{cor} \approx 2 \times 10^7 \left( \frac{\gamma_0}{10^4} \right)^{1/2} \left( \frac{\sin^3 \alpha}{\cos \alpha} \right)^{1/2}, \quad (14)$$

where the initial injection Lorentz factor has been normalized on  $10^4$  (e.g., Melrose 1998).

It is generally assumed that the high energy emission is generated by particles sliding along open field lines. In the framework of the present model, these field lines are almost straight in a sense that their curvature radius exceeds the nominal light cylinder radius. Yet, in the labora-

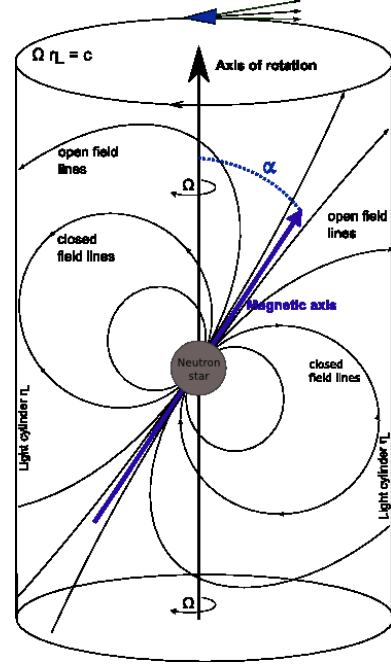


**Figure 2.** Sketch of the magnetospheric-centrifugal Pulsar model. Charged particles following co-rotating magnetic field lines will be radially decelerated while moving outwards but attain a large azimuthal velocity component close to light cylinder (LC) surface. A suitably aligned observer will see a strong (beamed) high-energy emission pulse for a short fraction of the period.

tory frame of reference particles will almost rigidly rotate on the LC surface (Gold 1969). Therefore, curvature emission (e.g., Ochelkov & Usov 1980) could be of significance in limiting the maximum attainable energies. For Lorentz factor of the order of  $\gamma \sim 10^7$  the characteristic peak frequency,  $\nu_{cur} \approx 3c\gamma^3/(4\pi R_c)$ , with  $R_c \simeq r_L$ , in the case of the Crab Pulsar becomes

$$\nu_{cur} \approx 5 \times 10^{22} \times \left( \frac{\gamma}{10^7} \right)^3 \text{ Hz}, \quad (15)$$

which corresponds to photon energies of the order of  $0.2 (\gamma/10^7)^3$  GeV. Hence curvature emission could in principle lead to a detectable, pulsed GeV contribution. Note that in principle some mild variation in curvature radii  $R_c$  may occur that could be determined within a more detailed approach (e.g., Thomas & Gangadhara 2007). We may estimate achievable energies in the presence of curvature losses by equating the associated cooling time scale  $t_{cur} = \gamma mc^2 / P_{cur}$ , where  $P_{cur} = 2e^2 c \gamma^4 / (3r_L^2)$  is the single particle curvature energy loss rate, i.e.

$$t_{cur} \approx 4.5 \times 10^{18} \times \frac{1}{\gamma^3} \text{ sec}, \quad (16)$$

with the acceleration timescale (i.e., eq. [4] with  $r_L$  replaced by  $r_l$ ) as applied to the Crab Pulsar,

$$t_{acc} \approx \frac{2.6 \times 10^{-3}}{\sin \alpha} \times \left( \frac{\gamma_0}{\gamma} \right)^{1/2} \text{ sec}, \quad (17)$$

yielding maximum attainable Lorentz factor

$$\gamma_{max}^{cur} \approx 5 \times 10^7 \sin^{2/5} \alpha, \quad (18)$$

where we have employed  $\gamma_0 \approx 10^4$ . Since  $\gamma_{max}^{cor} < \gamma_{max}^{cur}$ , the relevant constraint is thus essentially imposed by the requirement of co-rotation and not by curvature losses. In the approach described here, efficient particle acceleration is thus taking place in the LC zone, the energisation being mediated by centrifugal effects and not magnetic field-aligned electric fields (cf. also Hirotani 2014).

In the considered framework, the high energy radiation is generated in a thin shell of thickness

$$d \sim \gamma_0 r_L / \gamma \quad (19)$$

close to the LC surface (Osmanov & Rieger 2009). For a quasi-monoenergetic particle distribution the total luminosity could be approximated by  $L_{cur}^{GeV} \sim 2n_{GJ} M \Delta V P_{cur}$ , where  $\Delta V \sim \chi (\delta l)^2 d$  is the corresponding volume,  $\chi \lesssim 1$  is a dimensionless factor depending on the topology of magnetic field lines,  $\delta l \sim r_L \theta$  is the azimuthal length scale involved in this process,  $\theta \sim \Omega P / 10$  is the corresponding angle, where  $P / 10$  is an approximate value for the pulse duration inferred from the light curve observed (Ansoldi et al. 2016), and where we have taken into account that the pulsar emits in two channels. Combining the noted values, the pulsed luminosity generated due to curvature emission at energy  $h\nu_{cur}$  in the GeV band would be of the order of

$$L_{cur}^{GeV} \simeq 2 \times 10^{34} \left( \frac{\gamma}{10^7} \right)^4 \chi \cos \alpha \sin^3 \alpha \text{ erg/sec}. \quad (20)$$

The specific amount and the spectral shape will depend on the real (space-energy) distribution of particles and the range of curvature radii involved, and will need detailed modelling. Given the magnitude of eq. (20) and the fact that the emission is expected to be significantly focused (beamed; see also below), curvature radiation is likely to be of prime relevance for understanding the origin of the  $\gamma$ -ray emission as seen by Fermi-LAT (Abdo et al. 2010; Ansoldi et al. 2016).

Given the generic constraints for curvature emission (e.g., eq. [15]), it is usually believed that inverse Compton (IC) scattering is responsible for the VHE emission in millisecond pulsars (e.g., Lyutikov 2013; Harding & Kalapotharakos 2015; Ansoldi et al. 2016). To this, in principle a variety of soft photons fields could contribute, e.g. the thermal emission of the neutron star or secondary synchrotron emission. As shown in Osmanov & Rieger (2009), in the centrifugal-type approach following Gold (1969), the contribution of the star's thermal photon field to the IC process becomes of relevance as the particle-soft photon interaction angle is not negligible but of order  $\sim \pi/2$ . For the Crab pulsar, the surface temperature is of the order of  $T \simeq 1.2 \times 10^6$  K (e.g., Weisskopf et al. 2011), corresponding to photon energies of  $2.8kT \sim 0.3$  keV. IC up-scattering of thermal photons to the VHE regime will thus occur in the Klein-Nishina regime. One could verify that the associated electron inverse Compton losses will not impose further restrictions on the maximum attainable energies by recourse to the single particle emission power (e.g., Blumenthal & Gould 1970)

$$P_{KN} \simeq \frac{\sigma_T (mckT)^2}{16\hbar^3} \left( \ln \frac{4\gamma kT}{mc^2} - 1.981 \right) \left( \frac{r_s}{r_l} \right)^2, \quad (21)$$

where  $\sigma_T \approx 6.65 \times 10^{-25} \text{ cm}^2$  is the Thomson cross section,  $\hbar \approx 1.05 \times 10^{-27} \text{ erg-sec}$  is the Planck constant,

$k = 1.38 \times 10^{-16} \text{ erg/deg(K)}$  is the Boltzmann constant and  $r_s \approx 11.5 \text{ km}$  is the neutron star's radius (Lattimer 2012). To first order the corresponding cooling timescale  $t_{IC} = \gamma mc^2 / P_{KN}$  thus increases and becomes less constraining with Lorentz factor  $\gamma$ , whereas in contrast the acceleration timescale, eq. (4), decreases as  $1/\gamma^{1/2}$ . The noted IC scattering is thus not expected to impose constraints on the acceleration efficiency. Up-scattering of thermal photons could, however, lead to pulsed  $\gamma$ -ray emission in the VHE domain as pointed out in Osmanov & Rieger (2009). The scattered photons could well reach energies of the order of  $\epsilon \approx \gamma mc^2 \sim 5 (\gamma/10^7) \text{ TeV}$ . The MAGIC experiment has recently reported pulsed VHE emission with an energy flux level for the higher peak P2 of  $F = (9 \pm 3) \times 10^{-14} \text{ TeV cm}^{-2} \text{ s}^{-1}$  in the interval [965, 1497] GeV (Ansoldi et al. 2016), corresponding to an isotropic equivalent (spectral) luminosity of  $L_{TeV} \simeq (5 - 10) \times 10^{31} \text{ erg/s}$  at a distance of  $d \simeq 2 \text{ kpc}$ . In the considered framework, this emission would be generated by relativistic particles with Lorentz factors  $\sim (2 - 3) \times 10^6$ . We may again roughly estimate the possible order of magnitude for the spectral IC luminosity at  $\sim 1 \text{ TeV}$  expected in the centrifugal model by multiplying the single particle power  $P_{KN}$ , eq. (21), with the relevant particle number  $N \simeq 2n_{GJ} M \Delta V$  (two channels) to obtain

$$L_{IC}^{TeV} \simeq 1.4 \times 10^{31} \left( \frac{B}{10^6 \text{ G}} \right) \left( \frac{T}{1.2 \times 10^6 \text{ K}} \right)^2 \chi \cos \alpha \sin^2 \alpha \frac{\text{erg}}{\text{s}}. \quad (22)$$

One could use this expression to evaluate the degree of focusing and estimate a fiducial solid angle for the corresponding IC emission cone of  $\Delta\Omega \sim L_{IC}^{TeV} / (d^2 F) \sim 2.6 \chi \sin^2 \alpha \cos \alpha \text{ sr}$  if a dipolar field scaling  $B(r_l) \propto \sin^3 \alpha$  close to the LC surface is employed. In Fig. 2 a sketch of the magnetospheric-centrifugal Pulsar model is shown. Following the approach developed by Gold (1969) centrifugally accelerated particles in the LC zone have large azimuthal velocities and thus approximately emit along a tangent to the LC surface. It seems evident that in this approach the peaks in the light curves are in phase for all energy regimes that are rotationally produced sufficiently close to the LC area.

A priori, the radiating particle distribution is not expected to be mono-energetic, but instead to have some distribution in energy. This is a complicated issue and, amongst others, likely to be sensitive on the magnetic field topology, the injection spectrum and radiation reaction effects. Nevertheless, one can still evaluate some simple characteristics: Suppose electrons are injected (by inner gap-type processes) into the magnetosphere at a rate  $Q$  with some Lorentz factor  $\gamma_0$  and centrifugally accelerated along a magnetic field line until co-rotation breaks down and they escape further acceleration by crossing the LC surface. Then to first order, the differential particle density distribution  $n(\gamma)$  along a field line in the steady state can be approximated by (Rieger & Aharonian 2008)

$$n(\gamma) \simeq \frac{Q t_{acc}}{\gamma} H(\gamma - \gamma_0) \propto \gamma^{-3/2} \quad (23)$$

using that  $t_{acc} \propto \gamma^{-1/2}$ , eq. (4). Particles with higher  $\gamma$  are located closer to the LC surface and occupy a thinner shell of width  $d \propto \gamma_0 / \gamma$ , eq. (19), compared to those at lower energies. An observer will thus see the integrated emission produced by an effective particle number  $N = \int N(\gamma) d\gamma =$

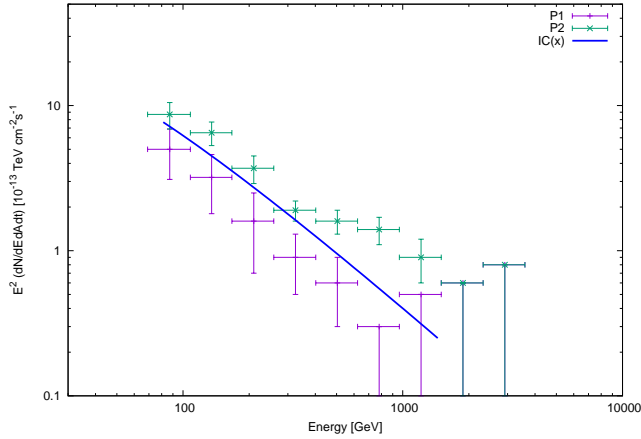


**Figure 3.** Illustration of the spectral VHE characteristics expected in the magneto-centrifugal Pulsar model as a result of inverse Compton scattering of thermal photons in the KN regime. The spectral points are the MAGIC (phase-folded) VHE measurements for the main pulse P1 and the interpulse P2, respectively (Ansoldi et al. 2016).

$\int n(\gamma) d\gamma dV = \int n(\gamma) \Delta V d\gamma$ , i.e., by an effective differential number of electrons  $dN_e = N_e(\gamma) d\gamma$  with a power-law distribution

$$N_e(\gamma) = n(\gamma) \Delta V \propto \gamma^{-5/2}, \quad (24)$$

noting that  $\Delta V \propto d \propto 1/\gamma$ . Up-scattering of a thermal black body distribution by a power law electron distribution with power index  $p$  in the KN limit will produce a photon spectrum (Blumenthal & Gould 1970)

$$\frac{dN_\gamma}{d\epsilon_\gamma dt} \propto \epsilon_\gamma^{-(p+1)} \left( \ln \frac{\epsilon_\gamma kT}{m^2 c^4} + 1 + C(p) \right) \quad (25)$$

for photon energies  $\epsilon_\gamma \ll \gamma_{max} m_e c^2$ , where  $C(p = 2.5) \simeq -2.4$ . The corresponding spectral characteristics resulting from the power law electron distribution  $p = 2.5$  of eq. (24) turns out to be surprisingly close to the VHE measurements by MAGIC, reporting photon indices  $\alpha = 3.5 \pm 0.1$  (for P1) and  $\alpha = 3.0 \pm 0.1$  (for P2). This is illustrated in Fig. 3. It is likely that modifications in, for example, the magnetic field topology and a detailed treatment of the particle injection and transport, aberration and travel time effects will lead to some index variation around this main spectral value but full modelling would be required to infer its plausible range.

## 4 CONCLUSIONS

The recent detection of pulsed VHE emission from the Crab Pulsar (Ansoldi et al. 2016) has opened new avenues in pulsar research. The apparent synchronisation of the pulse profile at GeV and TeV energies suggests a common property such as a very similar location of production, the transparency for  $\gamma$ -ray photons hints to an outer magnetospheric region, while the expected IC origin points to the presence of very energetic particles with Lorentz factors of at least  $\gamma \sim 5 \times 10^6$ . Such characteristics are challenging to accommodate in traditional emission models. In the present paper

we have argued that magneto-centrifugal particle acceleration may offer an interesting means to account for the noted characteristics. In this framework, efficient particle acceleration takes place in the vicinity of the light cylinder, with the high-energy  $\gamma$ -ray emission related to curvature radiation and the VHE emission (above some tens of GeV) generated by inverse Compton (IC) upscattering in the Klein-Nishina regime. The model assumes the occurrence of pair cascades as conventionally treated to provide the seed particles for injection. A simple analysis of the anticipated VHE spectral characteristics suggests a power-law index remarkably close to that actually observed. In the present model the slight spectral difference reported for the pulses P1 and P2 in the VHE regime could be related to two different magnetospheric locations with varying field topology along with possible variations in the injection spectrum. A full treatment of the corresponding particle transport and radiation properties, aberration and travel time effects seems required, however, to elucidate its most plausible range and to eventually help us understand particle acceleration processes in pulsar magnetospheres. Given the promising potential of magneto-centrifugal particle acceleration for understanding the origin of the observed VHE emission, this seems a program worth doing. The current MAGIC results rely on an analysis that combined many periods ( $\sim 320$ h, spread from 2007 to 2014) with different sensitivities and energy thresholds, in which the pulse P1 is detected with a moderate significance level of  $\leq 2.8\sigma$ . Updated VERITAS results (based on  $\sim 200$ h of data) find a phase-averaged differential spectrum for the Crab Pulsar compatible with the MAGIC results, but did not yet manage to establish pulsed emission above 400 GeV (Nguyen et al. 2015). Further observations with current and future (CTA) instruments (e.g., de Ona-Wilhelmi et al. 2013), establishing a homogeneous data set, and refined analysis will thus be important to better characterise its spectral evolution and extension, and thereby eventually help us to understand the origin of the high-energy emission in young pulsars.

## ACKNOWLEDGMENTS

The research of ZO was partially supported by the Shota Rustaveli National Science Foundation grant (N31/49). FRM acknowledges financial support by a DFG Heisenberg Fellowship (RI 1187/4-1).

## REFERENCES

- Abdo, A.A. et al. (Fermi-LAT Collaboration), 2010, *ApJ*, 708, 1254
- Abdo, A.A. et al. (Fermi-LAT Collaboration), 2013, *ApJS*, 208, 17
- Abramowicz, M. A. & Prasanna, A. R., 1990, *MNRAS*, 245, 729
- Aharonian, F. et al., 2004, *ApJ*, 614, 897
- Aharonian, F., Bogovalov, S. & Khargulyan, D., 2012, *ApJ*, 482, 507
- Aliu, E. et al. (VERITAS Collaboration) 2011, *Science*, 334, 69

- Ansoldi, S. et al. (MAGIC Collaboration), 2016, *A&A*, 585, 133
- Arons, J., 1983, *ApJ*, 266, 215
- Bednarek, W. 2012, *MNRAS*, 424, 2079
- Blumenthal, G.R. & Gould, R.J., 1970, *Rev. Mod. Phys.*, 42, 237
- Bogovalov, S. V., 2014, *MNRAS*, 443, 2197
- Bogovalov, S. V., 2001, *A&A*, 367, 159
- Cheng, K.S., Ho, C. & Ruderman, M.A., 1986, *ApJ*, 300, 500
- Chiang, J. & Romani, R.W., 1994, *ApJ*, 436, 754
- Daugherty, J.K., & Harding, A.K., 1982, *ApJ*, 252, 337
- de Ona-Wilhelmi, E. et al. (CTA Consortium), 2013, *APh*, 43, 287
- Dermer, C.D., & Sturmer, S.J., 1994, *ApJ*, 420, L75
- Gangadhara, R.T., 1996, *A&A*, 314, 853
- Gangadhara, R.T., & Lesch, H. 1997, *A&A*, 323, L45
- Ghisellini, G., Tavecchio, F., Bodo, G. & Celotti, A. 2009, *MNRAS*, 393, L16
- Gold, T., 1969, *Nature*, 221, 25
- Goldreich, P. & Julian, W.H., 1969, *ApJ*, 157, 869
- Gudavadze, I., Osmanov, Z. & Rogava, A., 2015, *IJMPD*, 24, 1550042
- Harding, A. K., & Kalapotharakos, C. 2015, *ApJ*, 811, 63
- Hirotsu, K. 2007, *ApJ* 662, 1173
- Hirotsu, K. 2014, *MNRAS*, 442, L43
- Machabeli, G.Z. & Rogava, A.D., 1994, *Phys. Rev. A*, 50, 98
- Melrose, D. B., 1998, *Proc. of APPTC97 (Toki, Japan)*, ed. Y. Tomita et al., 96
- Michel, F. C. 1991, *Theory of Neutron Star Magnetospheres* (Univ. of Chicago Press)
- Mochol, I., & Pétri, J. 2015, *MNRAS*, 449, L51
- Muslimov, A.G., & Tsygan, A.I., 1992, *MNRAS*, 255, 61
- Nguyen, T.J. et al. (for the VERITAS Collaboration), 2015, *Proc. 34th ICRC (The Hague)*, PoS(ICRC2015)828
- Lattimer, J.M., 2012, *Annu. Rev. Nucl. Part. Sci.*, 62, 485
- Lemoine-Goumard, M., 2015, *Proc. 34th ICRC 2015 (The Hague)*, PoS(ICRC2015)012
- Lyutikov, M. 2013, *MNRAS*, 431, 2580
- Lyne, A.G. et al., 2015, *MNRAS*, 446, 857
- Ochelkov Yu. P. & Usov V.V. 1980, *Ap&SS* 69, 439
- Osmanov, Z. & Rieger, F.M., 2009, *A&A* 502, 15
- Osmanov, Z., Rogava, A. S. & Bodo, G., 2007, *A&A*, 470, 395
- Rieger, F.M., 2011, *IJMPD*, 20, 1547
- Rieger, F.M., & Aharonian, F., 2008, *A&A*, 479, L5
- Rieger, F.M., & Mannheim, K., 2000, *A&A*, 353, 473
- Rogava, A.D., Dalakishvili, G. & Osmanov, Z., 2003, *Gen. Rel. and Grav.*, 35, 1133
- Ruderman, A., & Sutherland, P. G., 1975, *ApJ*, 196, 51
- Thomas, R.M.C., & Gangadhara, R.T., 2007, *A&A*, 467, 911
- Usov, V.V. & Shabad, A., 1985, *Ap&SS*, 117, 309
- Shapiro, S.L., & Teukolsky, S.A., *Black Holes, White Dwarfs and Neutron Stars*, Chapter 5, Wiley 2004
- Weekes, T. C., Cawley, M. F., Fegan, D. J., et al. 1989, *ApJ*, 342, 379
- Weisskopf, M.C. et al., 2011, *ApJ*, 743, 139
- Xu, Y.D., 2002, *A&A*, 381, 357